

www.chemeurj.org

# An Adaptive Hydrogen-Bonded Organic Framework for the Exclusive Recognition of p-Xylene

Li Ma<sup>+</sup>,<sup>[a]</sup> Yi Xie<sup>+</sup>,<sup>[a]</sup> Rebecca Shu Hui Khoo,<sup>[b]</sup> Hadi Arman,<sup>[a]</sup> Bin Wang,<sup>[a]</sup> Wei Zhou,<sup>[c]</sup> Jian Zhang,<sup>[b]</sup> Rui-Biao Lin,<sup>[d]</sup> and Banglin Chen<sup>\*[a]</sup>

**Abstract:** Separation of xylene isomers is one of the most important but most challenging and energy-intensive separation processes in the petrochemical industry. Here, we report an adaptive hydrogen-bonded organic framework (HOF-29) constructed from a porphyrin based organic building block 4,4',4'''-(porphyrin-5,10,15,20-tetrayl) tetrabenzonitrile (PTTBN), exhibiting the exclusive molecular recognition of *p*-xylene (pX) over its isomers of *o*-xylene (oX) and *m*-xylene

(mX), as clearly demonstrated in the single crystal structure transformation and  $^1H$  NMR studies. Single crystal structure studies show that single-crystal-to-single-crystal transformation from the as-synthesized HOF-29 to the pX exclusively included HOF-29  $\supset$  X is triggered by the encapsulation of pX molecules, accompanied by sliding of the 2D layers and local distortion of the ligand, which provides multiple C–H··· $\pi$  interactions.

Separation of benzene derivatives from each other, as one of the seven key separation processes, have been recognized to reap global benefits.[1] Among all the benzene derivatives, C8 isomer separations play a great role in the chemical industry to produce valuable feedstocks. Because these C8 isomers have similar physical and chemical properties as shown in their similar boiling points and molecular sizes, it is very challenging but very important to develop environmentally benign and low-cost materials for these separations to replace the industrially implemented energy extensive separation technology of the cryogenic distillation. [2,3] Among these isomers, pX, the raw material to produce terephthalic acid, which has been widely used for the production of polyethylene terephthalate (PET) and polyester, is the most valuable xylene isomer chemical.<sup>[4]</sup> The microporous materials developed over the past three decades, including metalorganic frameworks/porous coordination polymers (MOFs/PCPs), [5-13] covalent organic frameworks (COFs), [14] metalorganic and/or pure organic complexes/cages, [15-20] have principally provided the resolution of the finely pore tuning and engineering for the selective separation of xylene isomers. Although extensive efforts have been pursued to target such microporous materials for this very important separation, highly pX-selective porous adsorbents have been barely realized. [21,22] In fact, most of the discovered porous materials for these separations show the co-adsorption of the other isomers though the materials take up more pX over others.

Compared with MOFs and COFs for different molecular separations and recognitions; hydrogen-bonded organic frameworks, as a new kind of microporous materials, have been much less explored though some HOF materials have been recently realized for their diverse functions and applications. [23-31] HOFs are generally more flexible than other microporous materials, which might provide more driving forces to developing adaptive microporous materials for some challenging separation, as shown in our recent example of HOFs for the highly selective  $C_2H_4/C_2H_6$  separation at the elevated temperature. [32] HOFs also have some uniqueness in terms of their solution processability, straightforward recrystallization and regeneration, providing the bright promise of HOFs for diverse separation applications.[33-37] Herein we report a microporous HOF-29 constructed from the organic building block 4,4',4",4"'-(porphyrin-5,10,15,20-tetrayl) tetrabenzonitrile (PTTBN). The synthesis of the organic linker was provided in the Supporting Information. (Figure S1) Diffusion of dichloromethane (DCM) into the DMF/DMSO solution of PTTBN readily formed HOF-29. Single-crystal X-ray diffraction studies revealed that HOF-29 crystallizes in the triclinic  $P\bar{1}$ space group with half of a PTTBN and one DMF molecule in the asymmetric unit. (Table S1). In the crystal structure of HOF-29, each PTTBN linker is connected with four adjacent

- [a] L. Ma,<sup>+</sup> Y. Xie,<sup>+</sup> Dr. H. Arman, Dr. B. Wang, Prof. B. Chen Department of Chemistry University of Texas at San Antonio One UTSA Circle, San Antonio, Texas 78249-0698 (USA) E-mail: banglin.chen@utsa.edu
- [b] R. S. H. Khoo, Dr. J. Zhang Organic and Macromolecular Synthesis Facility Molecular Foundry Lawrence Berkeley National Laboratory One Cyclotron Road, MS 67R6110, Berkeley, CA 94720 (USA)
- [c] Dr. W. Zhou NIST Center for Neutron Research National Institute of Standards & Technology Gaithersburg, Maryland 20899-6102 (USA)
- [d] Dr. R.-B. Lin MOE Key Laboratory of Bioinorganic and Synthetic Chemistry School of Chemistry Sun Yat-Sen University Guangzhou 510006 (P. R. China)
- [+] These Authors contributed equally to this work.
- Supporting information for this article is available on the WWW under https://doi.org/10.1002/chem.202104269



linkers via four pairs of intermolecular C–H···NC hydrogen bonds (H···N 2.529–2.606 Å, C–H···N 3.423–3.530 Å) to form a two-dimensional sql network, which runs across crystallographic ( $12\bar{2}$ ) plane. (Figure 1a). The adjacent PTTBN molecules from two layers were packed compactly through multiple hydrogen bonding interactions (H···N 2.641–2.830 Å, C–H···N 3.487–3.568 Å) and slipped  $\pi$ - $\pi$  stacking interactions with a distance of 3.761 Å, which lead to an inclined AA stacking pattern (Figure 1b, 1d and S2a). Such packing fashion allows the intrinsic cavity embedded within the sql network to interconnect to generate a one-dimensional channel running along a-axis (cavity and aperture size:  $12.7 \times 6.3 \times 4.1$  Å $^3$ ,  $9.1 \times 3.7$  Å $^2$ ) with a void ratio of 25.3% (Figure S3).

The purity of HOF-29 was confirmed by powder X-ray diffraction (PXRD) (Figure S4). Thermogravimetric analysis (TGA) showed that all the DMF guest molecules were lost at  $150\,^{\circ}\text{C}$  with a weight loss of 7.4%, while the plateau was maintained up to  $400\,^{\circ}\text{C}$  (Figure S5).

The ellipsoidal cavities within HOF-29 seem to be large enough to accommodate xylene molecules, so we investigated the molecular recognition behavior of HOF-29 towards xylenes. HOF-29 was first soaked in the commercial xylene mixture of isomers (ACS assay, > 98.5 %), composed of pX, oX, mX and EB (ethylbenzene), and then collected after thorough rinsing with hexane as the HOF-29 Duests. 1H NMR spectra of the resulting HOF-29 Duests in DMSO revealed that only pX molecules have been included into the cavities of HOF-29 Guests, as clearly shown in the characteristic <sup>1</sup>H NMR peak of the pX at 7.05 ppm (Figure 2a-b), so we retermed it as HOF-29 pX. It is very encouraging that the resulting HOF-29 pX keep high crystallinity, which allowed us to determine its crystal structure by synchrotron diffraction studies. Single-crystal synchrotron diffraction analysis showed that HOF-29⊃pX keeps the triclinic P1̄ space group, with a volume shrinkage of 6.5%, including 30.5% expansion of a-axis, 3.2% shrinkage of b-axis and 19.7% shrinkage of caxis. (Table S2) Only one crystallographically unique pX molecule was identified in the pore channel. Compared to the as-synthesized HOF-29 structure, after the inclusion of pX, stronger hydrogen bonding interactions between adjacent PTTBN molecules in the same sql net (N···H 2.527-2.580 Å, N···H–C 3.325–3.483 Å) were observed, while the

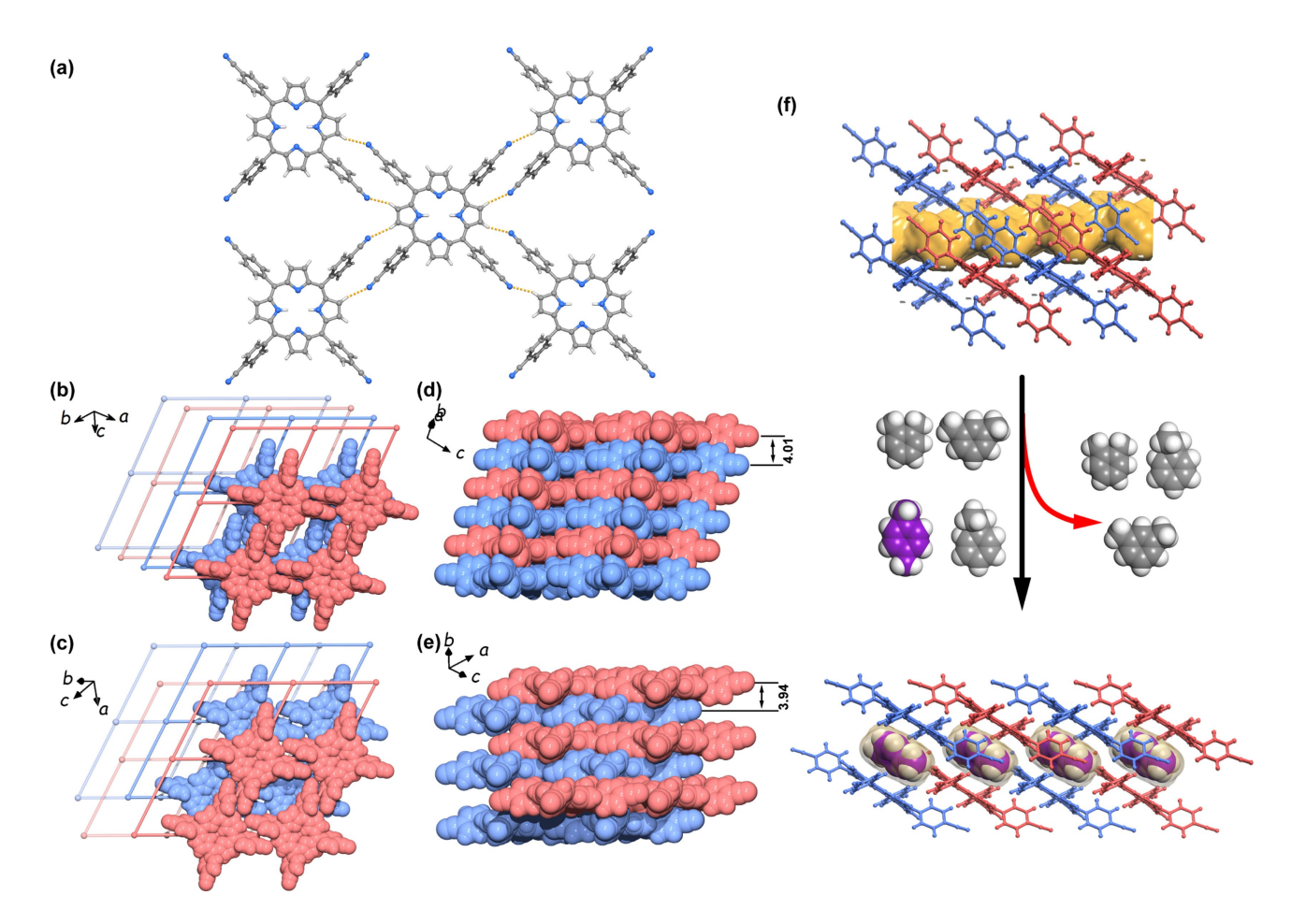


Figure 1. (a) Perspective view of the adjacent building blocks PTTBN in HOF-29, which are extended by intermolecular C-N···H hydrogen bonding (highlighted in yellow) into sql net. Grey, carbon; blue, nitrogen; white, hydrogen. Layer packing diagrams of HOF-29 (b) and HOF-29  $\supset$ pX (c) viewed perpendicularly to the layers, with simplified topology, showing different inclined AA and AB stacking patterns, respectively. Side views of HOF-29 (d) and HOF-29  $\supset$ pX (e) with interlayer distance indicated. The guest solvent molecules are omitted for clarity. (f) Schematic representation of adaptive structural transformation from HOF-29 to HOF-29  $\supset$ pX driven by the specific recognition of pX.

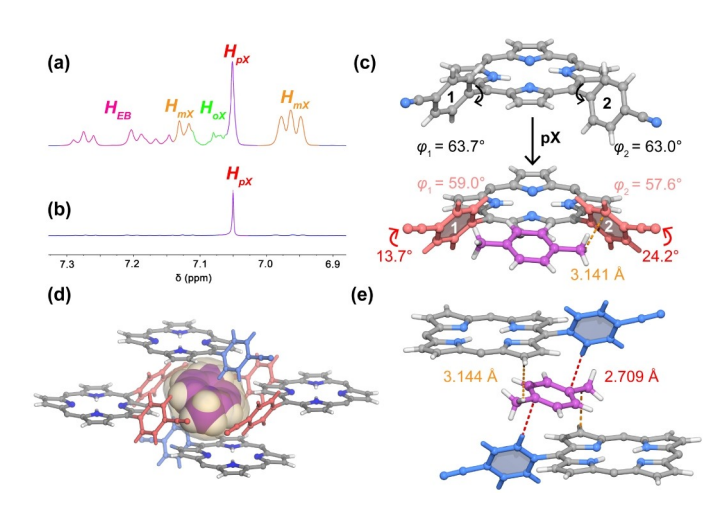


Figure 2. ¹H NMR spectra of (a) commercial xylenes isomers (ACS assay, >98.5%) containing mX (orange), oX (green) and pX (purple), EB (magenta), and (b) HOF-29⊃pX in the DMSO- $d_6$  solution. (c) Comparison of the geometry of PTTBN in HOF-29 (top) and HOF-29⊃pX (bottom) with C–H···π interactions and dihedral angle (φ) between phenyl ring and porphyrin ring highlighted. (d) Perspective view of preferential binding configuration and pore confinement for pX in HOF-29⊃pX. The pX molecule is highlighted in CPK model. (e) The close C–H···π(pX)/π(porphyrin) contacts with the frameworks from top and bottom layers. Strong (H···π < 2.90 Å) and weak (H···π > 2.90 Å) interactions are displayed in red and orange, respectively.

interlayer distance was decreased from 4.01 Å to 3.94 Å (Figure 1c and 1e). The layers in HOF-29⊃pX were further inclined to form the AB packing pattern in which the interlayer stacking of PTTBN molecules was slide, resulting in a loss of  $\pi$ - $\pi$  stacking interactions and elongated hydrogen bonding interactions (H ···N 2.650-2.870 Å, C-H···N 3.497-3.568 Å) (Figure S2b). Therefore, the one-dimensional pore channels in HOF-29 were transformed into discrete cavities with a size of 11.1×7.0×4.7 ų in HOF-29⊃pX due to the sliding of layers, which encapsulates one pX molecule, corresponding to one pX per PTTBN (Figure 1f and S7). A close examination of the crystal structures reveals that tilting and bending of phenyl ring in PTTBN linkers, compared to the as synthesized one, were found to realize the optimal binding and maximized contacts for the pX molecules: the dihedral angel between phenyl ring (ring 1 and 2) and porphyrin ring decreased from  $63.7^{\circ}$  and  $63.0^{\circ}$  to  $59.0^{\circ}$  and 57.6°, respectively, while the phenyl rings were bent by 13.7° and 24.7°, respectively (Figure 2c). As a result, the pX molecules were confined within the cavities in a sandwichedlike fashion through multiple hydrogen bonding interactions mainly strong C–H··· $\pi$ (pX) interactions with the phenyl ring with a distance of 2.709 Å (shorter than 2.90 Å, sum of vdW radii of C and H), accompanied by weak C–H $\cdots\pi$ (phenyl)/  $\pi$ (porphyrin) interactions (3.141 and 3.144 Å) (Figure 2c–e and S8). The crystallographic studies further confirmed the adaptive nature of the pore structure and conformation of linkers in HOF-29 for its exclusive recognition of pX molecules.

To further explore the potential of HOF-29 for its specific recognition of pX molecules from C8 isomers, we further

individually examined its recognition behaviors in binary mX/oX (volumetric 1:1), mX/pX (1:1) and oX/pX (1:1), and ternary mX/oX/pX (1:1:1) mixtures, respectively. Interestingly, HOF-29 does not recognize either mX and oX at all even without the existence of pX, as clearly shown in Figure 3a in which only the characteristic <sup>1</sup>H NMR peaks of organic linker PTTBN (8.86 ppm, singlet; 8.43 ppm, doublet; 8.32 ppm, doublet) were observed. As expected, when soaking HOF-29 into the mX/pX (1:1), oX/pX (1:1), and ternary mX/oX/pX (1:1:1) mixtures, only pX molecules were exclusively included in the resulting HOF-29 pX solids (Figure 3b-d and S9-11). As mentioned above, the 1D channels within the as-synthesized HOF-29 are large enough to encapsulate all the mX, oX and pX molecules. However, the weak interactions between mX/oX with the framework, which are even weaker than the interactions between the DMF molecules in the as-synthesized HOF-29 with the framework. The driving force for the structural transformation from the 1D channel based framework of HOF-29 to the framework of HOF-29 pX with the isolated cavitities is the slightly stronger interactions between pX molecules and the HOF framework.

In summary, we have successfully constructed a novel microporous HOF, HOF-29, from a simple organic molecule. This HOF exbibits exclusive recognition of pX over mX, oX and EB, as clearly established in both molecular recognition studies and single-crystal diffraction experiments. The flexible and thus more adaptable nature of HOF materials, compared with those well-developed ones such as MOF and COFs,

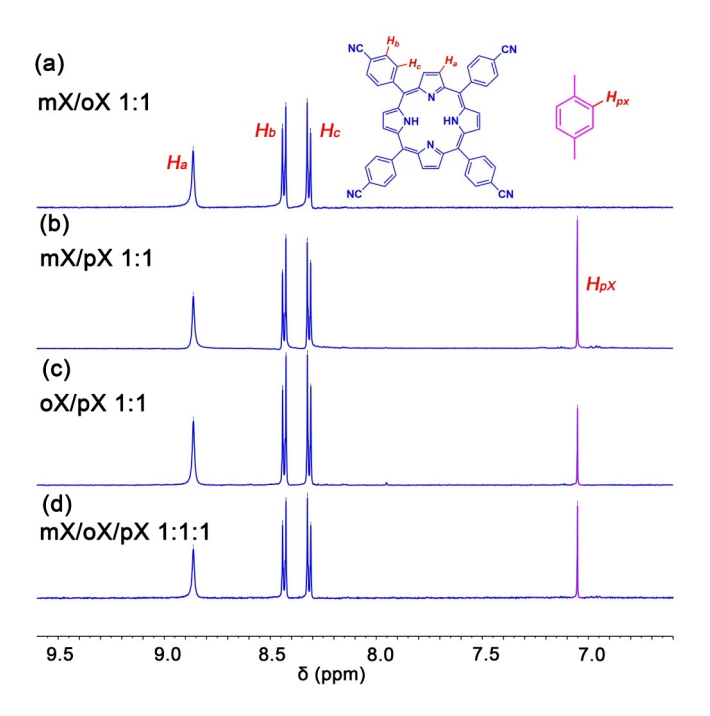


**Figure 3.** <sup>1</sup>H NMR spectra of HOF-29 $\supset$ Guests in the DMSO- $d_6$  solution. The HOF-29 $\supset$ Guests were collected after soaking in binary (a) mX/oX (1:1), (b) mX/pX (1:1) and (c) oX/pX (1:1), and (d) ternary mX/oX/pX (1:1:1) mixtures, respectively, followed by thorough rinsing by hexane solvents.



might not only for us to mimic these porous materials but also to enable us to target some unusual HOFs with superior and unexpected performance. We are now working on the construction of more HOF materials for diverse applications and functions.

#### **Experimental Section**

Crystallization of HOF-29: PTTBN (72.2 mg) was dissolved in DMF/DMSO (6 mL/6 mL) after sonication and filtration. The resultant clear solutions were divided into fifteen 4-mL open vials. DCM was carefully layered on the top of the solution, which were allowed to slowly diffuse into the DMF/DMSO solution of PTTBN at room temperature. Purple-red crystals were isolated in the bottom of the vials after two weeks.

Molecular recognition experiments: 10 mg of HOF crystals were soaked in 2 mL of mixture of xylene isomers for 2 days. The crystals were isolated by centrifugation and rinsed with 5 mL of hexane for 5 times. The samples were dried in air and applied under low vacuum for about 3 h. The crystals were completely dissolved in DMSO- $d_6$  after vigorous sonication and heating for  $^1\text{H}$  NMR spectra measurements.

Deposition Numbers 2121390 (for HOF-29), 2121391 (for HOF-29 ⊃pX) contain the supplementary crystallographic data for this paper. These data are provided free of charge by the joint Cambridge Crystallographic Data Centre and Fachinformationszentrum Karlsruhe Access Structures service.

## Acknowledgements

We greatly acknowledge support from Welch Foundation (AX-1730). L. M. thanks the generous support from the Presidential Distinguished Research Fellowship (PDRF) of the University of Texas at San Antonio (UTSA). R.-B. L. thanks the support from NSFC (22101307). X-ray diffraction experiments conducted at UTSA was supported by the U.S. National Science Foundation (MRI 1920057). X-ray diffraction studies at the Molecular Foundry and Advanced Light Source was supported by the Office of Science, Office of Basic Energy Sciences, of the U.S. Department of Energy (DE-AC02-05CH11231).

#### Conflict of Interest

The authors declare no conflict of interest.

### **Data Availability Statement**

The data that support the findings of this study are available in the supplementary material of this article.

**Keywords:** hydrogen-bonded organic framework  $\cdot$  microporous materials  $\cdot$  *p*-xylene recognition

[1] D. S. Sholl, R. P. Lively, *Nature* **2016**, *532*, 435–437.

- [2] M. Minceva, A. E. Rodrigues, AIChE J. 2007, 53, 138-149.
- [3] K. Ziegler-Skylakakis, J. Fabri, U. Graeser, T. A. Simo, Xylenes, in Ullmann's Encyclopedia of Industrial Chemistry, Wiley-VCH, 2019, pp. 1–20.
- [4] Y. Yang, P. Bai, X. Guo, Ind. Eng. Chem. Res. 2017, 56, 14725-14753.
- [5] A. Torres-Knoop, R. Krishna, D. Dubbeldam, Angew. Chem. Int. Ed. 2014, 53, 7774–7778; Angew. Chem. 2014, 126, 7908–7912.
- [6] J. M. Holcroft, K. J. Hartlieb, P. Z. Moghadam, J. G. Bell, G. Barin, D. P. Ferris, E. D. Bloch, M. M. Algaradah, M. S. Nassar, Y. Y. Botros, K. M. Thomas, J. R. Long, R. Q. Snurr, J. F. Stoddart, J. Am. Chem. Soc. 2015, 137, 5706–5719.
- [7] S.-Q. Wang, S. Mukherjee, E. Patyk-Kaźmierczak, S. Darwish, A. Bajpai, Q.-Y. Yang, M. J. Zaworotko, Angew. Chem. Int. Ed. 2019, 58, 6630–6634;
  Angew. Chem. 2019, 131, 6702–6706.
- [8] X. Yang, H.-L. Zhou, C.-T. He, Z.-W. Mo, J.-W. Ye, X.-M. Chen, J.-P. Zhang, Research 2019, 2019, 9463719.
- [9] X. Cui, Z. Niu, C. Shan, L. Yang, J. Hu, Q. Wang, P. C. Lan, Y. Li, L. Wojtas, S. Ma, H. Xing, Nat. Commun. 2020, 11, 5456.
- [10] X. Li, J. Wang, N. Bai, X. Zhang, X. Han, I. da Silva, C. G. Morris, S. Xu, D. M. Wilary, Y. Sun, Y. Cheng, C. A. Murray, C. C. Tang, M. D. Frogley, G. Cinque, T. Lowe, H. Zhang, A. J. Ramirez-Cuesta, K. M. Thomas, L. W. Bolton, S. Yang, M. Schröder, *Nat. Commun.* 2020, 11, 4280.
- [11] F. Vermoortele, M. Maes, P. Z. Moghadam, M. J. Lennox, F. Ragon, M. Boulhout, S. Biswas, K. G. M. Laurier, I. Beurroies, R. Denoyel, M. Roeffaers, N. Stock, T. Düren, C. Serre, D. E. De Vos, J. Am. Chem. Soc. 2011, 133, 18526–18529.
- [12] M. Lusi, L. J. Barbour, Angew. Chem. Int. Ed. 2012, 51, 3928–3931; Angew. Chem. 2012, 124, 3994–3997.
- [13] J. E. Warren, C. G. Perkins, K. E. Jelfs, P. Boldrin, P. A. Chater, G. J. Miller, T. D. Manning, M. E. Briggs, K. C. Stylianou, J. B. Claridge, M. J. Rosseinsky, Angew. Chem. Int. Ed. 2014, 53, 4592–4596; Angew. Chem. 2014, 126, 4680–4684.
- [14] J. Huang, X. Han, S. Yang, Y. Cao, C. Yuan, Y. Liu, J. Wang, Y. Cui, J. Am. Chem. Soc. 2019, 141, 8996–9003.
- [15] N. Sun, S.-Q. Wang, R. Zou, W.-G. Cui, A. Zhang, T. Zhang, Q. Li, Z.-Z. Zhuang, Y.-H. Zhang, J. Xu, M. J. Zaworotko, X.-H. Bu, *Chem. Sci.* 2019, 10, 8850–8854.
- [16] B. Moosa, L. O. Alimi, A. Shkurenko, A. Fakim, P. M. Bhatt, G. Zhang, M. Eddaoudi, N. M. Khashab, Angew. Chem. Int. Ed. 2020, 59, 21367–21371; Angew. Chem. 2020, 132, 21551–21555.
- [17] G. Zhang, A.-H. Emwas, U. F. Shahul Hameed, S. T. Arold, P. Yang, A. Chen, J.-F. Xiang, N. M. Khashab, Chem 2020, 6, 1082–1096.
- [18] K. Jie, M. Liu, Y. Zhou, M. A. Little, A. Pulido, S. Y. Chong, A. Stephenson, A. R. Hughes, F. Sakakibara, T. Ogoshi, F. Blanc, G. M. Day, F. Huang, A. I. Cooper, J. Am. Chem. Soc. 2018, 140, 6921–6930.
- [19] T. Mitra, K. E. Jelfs, M. Schmidtmann, A. Ahmed, S. Y. Chong, D. J. Adams, A. I. Cooper, *Nat. Chem.* **2013**, *5*, 276–281.
- [20] M. du Plessis, V. I. Nikolayenko, L. J. Barbour, J. Am. Chem. Soc. 2020, 142, 4529–4533.
- [21] Z. Zhang, S. B. Peh, C. Kang, K. Chai, D. Zhao, EnergyChem 2021, 3, 100057.
- [22] G. Zhang, Y. Ding, A. Hashem, A. Fakim, N. M. Khashab, Cell Rep. Phys. Sci. 2021, 2, 100470.
- [23] R.-B. Lin, Y. He, P. Li, H. Wang, W. Zhou, B. Chen, Chem. Soc. Rev. 2019, 48, 1362–1389.
- [24] W. Gong, D. Chu, H. Jiang, X. Chen, Y. Cui, Y. Liu, Nat. Commun. 2019, 10, 600.
- [25] K. Ma, P. Li, J. H. Xin, Y. Chen, Z. Chen, S. Goswami, X. Liu, S. Kato, H. Chen, X. Zhang, J. Bai, M. C. Wasson, R. R. Maldonado, R. Q. Snurr, O. K. Farha, Cell Rep. Phys. Sci. 2020, 1, 100024.
- [26] J. Luo, J.-W. Wang, J.-H. Zhang, S. Lai, D.-C. Zhong, CrystEngComm 2018, 20, 5884–5898.
- [27] I. Hisaki, C. Xin, K. Takahashi, T. Nakamura, Angew. Chem. Int. Ed. 2019, 58, 11160–11170; Angew. Chem. 2019, 131, 11278–11288.
- [28] T.-H. Chen, I. Popov, W. Kaveevivitchai, Y.-C. Chuang, Y.-S. Chen, O. Daugulis, A. J. Jacobson, O. Š. Miljanić, Nat. Commun. 2014, 5, 5131.
- [29] P. Brunet, M. Simard, J. D. Wuest, J. Am. Chem. Soc. 1997, 119, 2737– 2738.
- [30] J.-f. Feng, T.-F. Liu, R. Cao, Angew. Chem. Int. Ed. 2020, 59, 22392–22396; Angew. Chem. 2020, 132, 22578–22582.
- [31] A. Pulido, L. Chen, T. Kaczorowski, D. Holden, M. A. Little, S. Y. Chong, B. J. Slater, D. P. McMahon, B. Bonillo, C. J. Stackhouse, A. Stephenson, C. M. Kane, R. Clowes, T. Hasell, A. I. Cooper, G. M. Day, *Nature* 2017, 543, 657–664.



- [32] Y. Yang, L. Li, R.-B. Lin, Y. Ye, Z. Yao, L. Yang, F. Xiang, S. Chen, Z. Zhang, S. Xiang, B. Chen, *Nat. Chem.* 2021, 13, 933–939.
- [33] Y.-L. Li, E. V. Alexandrov, Q. Yin, L. Li, Z.-B. Fang, W. Yuan, D. M. Proserpio, T.-F. Liu, J. Am. Chem. Soc. 2020, 142, 7218–7224.
- [34] X. Zhang, L. Li, J.-X. Wang, H.-M. Wen, R. Krishna, H. Wu, W. Zhou, Z.-N. Chen, B. Li, G. Qian, B. Chen, J. Am. Chem. Soc. 2020, 142, 633–640.
- [35] F. Hu, C. Liu, M. Wu, J. Pang, F. Jiang, D. Yuan, M. Hong, Angew. Chem. Int. Ed. 2017, 56, 2101–2104; Angew. Chem. 2017, 129, 2133– 2136.
- [36] X.-Z. Luo, X.-J. Jia, J.-H. Deng, J.-L. Zhong, H.-J. Liu, K.-J. Wang, D.-C. Zhong, J. Am. Chem. Soc. 2013, 135, 11684–11687.

[37] Z. Bao, D. Xie, G. Chang, H. Wu, L. Li, W. Zhou, H. Wang, Z. Zhang, H. Xing, Q. Yang, M. J. Zaworotko, Q. Ren, B. Chen, J. Am. Chem. Soc. 2018, 140, 4596–4603

Manuscript received: November 30, 2021 Accepted manuscript online: January 4, 2022 Version of record online: January 27, 2022

[Correction added on February 21, 2022, after first online publication: Figure 1 and the Table of Contents image were changed to correctly display the structure of ethylbenzene]